Journal of Inflammation Research

Dovepress
Taylor & Francis Group

Open Access Full Text Article

ORIGINAL RESEARCH

Transcriptome Sequencing Reveals the Molecular Mechanism of Heat Stroke-Induced Myocardial Injury

Jie Xiang[1,2,*], Shijie Shao[1,2,*], Jie Huang[3], Na Yang[1,2], Fei Guo[4], Baopeng Tang[1,2], Ling Zhang[1,2]

[1]Xinjiang Key Laboratory of Cardiac Electrophysiology and Remodeling, Clinical Medical Research Institute, The First Affiliated Hospital of Xinjiang Medical University, Urumqi, People's Republic of China; [2]Department of Pacing and Electrophysiology, The First Affiliated Hospital of Xinjiang Medical University, Urumqi, People's Republic of China; [3]Institute of Cardiovascular Research, Southwest Medical University, Luzhou, Sichuan, People's Republic of China; [4]Department of Cardiology, The First Affiliated Hospital of USTC, Division of Life Sciences and Medicine, University of Science and Technology of China, Hefei, People's Republic of China

*These authors contributed equally to this work

Correspondence: Ling Zhang; Baopeng Tang, Department of Pacing and Electrophysiology, The First Affiliated Hospital of Xinjiang Medical University, 137 Liyushan Road, Urumqi, Xinjiang, 830000, People's Republic of China, Email ydzhangling@126.com; tangbaopeng1111@163.com

Background: The annual rise of global temperature and the continuous occurrence of extremely high temperatures in summer have significantly increased the incidence of heat stroke (HS), which has caused serious burden on the cardiovascular system. The purpose of this study was to investigate the potential mechanisms of heat stroke-induced myocardial injury via transcriptome sequencing.

Methods: HS models of rat and H9C2 cells were constructed and transcriptomic sequencing was performed. Bioinformatics methods were used to analyze transcriptomics to reveal the pathophysiological mechanism of HS-induced myocardial injury. Subsequently, machine learning was utilized to identify key targets of HS-induced myocardial injury. Finally, experiments such as Western blotting, flow cytometry and immunofluorescence were used to validate in vivo and in vitro.

Results: HS rats exhibited severe cardiac dysfunction. Transcriptomics revealed that HS-induced myocardial injury mainly involved apoptosis and inflammation. Meanwhile, there were significant differences in the expression of mitochondria-related genes, which were significantly enriched in the apoptosis pathway. Through machine learning, Jun was identified as a key target for HS-induced myocardial injury. In HS rat myocardial tissue, mitochondrial structure was severely disrupted, and Jun protein expression and cardiomyocyte apoptosis were significantly increased. In cell experiments, inhibition of Jun expression with Jun inhibitors (SR11302) significantly improved mitochondrial membrane potential and reduced cell apoptosis.

Conclusion: Our findings suggested that Jun-mediated mitochondrial apoptosis plays an important role in HS-induced myocardial injury, which provides a new preventive and therapeutic target for HS-induced myocardial injury.

Keywords: heat stroke, myocardial injury, apoptosis, jun, transcriptomics

Introduction

With the dramatic increase in global temperatures and the persistence of extremely high temperatures in summer, there has been a significant increase in morbidity and mortality from heat stroke (HS) and a consequent increase in heat-related illnesses.[1,2] HS is defined as a rapid increase in core temperature >40°C accompanied by systemic inflammatory response and multiple organ dysfunction syndrome.[3,4] The regulation of cardiovascular system plays a key role in the pathogenesis of HS. During HS, the cardiovascular system is involved in the whole body heat dissipation response and organ perfusion. However, the large volume of blood pumped from the heart into the peripheral vasculature can lead to hyperthermia and dehydration, reduced circulating blood volume, inadequate tissue perfusion, hypoxia, and necrosis of cardiomyocyte.[5,6] Therefore, the heart, as a heat-sensitive organ,[7,8] is more susceptible to myocardial injury, heart failure and arrhythmias in HS.[6,9,10]

Received: 13 January 2025
Accepted: 12 June 2025
Published: 19 June 2025

The mechanism of HS-induced myocardial injury has been widely discussed. The first is the imbalance between pro-inflammatory and anti-inflammatory. To some extent, the pathogenesis of HS is very similar to sepsis.[11] During HS, the body releases large amounts of cytokines, such as tumour necrosis factor-alpha (TNF-α) and interleukin-1β (IL-1β),[12,13] and stimulates neutrophil migration and adhesion, leading to dysregulation of pro-inflammatory and anti-inflammatory factors and inducing inflammatory cascade responses, which in turn lead to tissue damage.[14] Previous studies have shown that suppressing the inflammatory response is one of the effective therapies for HS-induced myocardial injury.[15,16] Secondly, HS causes abnormal cardiomyocyte death. The cardiotoxic effects of HS have been shown to be manifested in abnormal cardiomyocyte death, including apoptosis, necrosis and ferroptosis,[17,18] which may be partly related to disruption of mitochondrial structure and function. Because abnormal mitochondrial alterations have been observed in cardiomyocytes of HS rats.[19] In addition, metabolic abnormalities, endothelial cell damage and dysfunction and heat shock protein dysregulation have been highlighted in HS-induced myocardial injury.[6] However, despite numerous research efforts to explore the pathogenesis of HS, the mechanism of HS-induced myocardial injure remains unclear, and intervention and therapeutic targets are lacking.

In recent years, with the continuous development of life sciences, a variety of high-throughput omics technologies, including transcriptomics, proteomics and metabolomics, have been increasingly applied to the early diagnosis of diseases and the exploration of the pathophysiological mechanisms of diseases,[20] among which transcriptomics has been applied earlier and is the most widely used.[21] Compared with traditional physiology-based or "star molecule" studies, high-throughput techniques for pathway analysis of co-regulatory genes and identification of functional groups provide the possibility to search for new key molecules.[22] Many studies have applied omics to heat stroke. For example, Fang et al used multi-omics analyses to explore the molecular mechanisms of HS-induced cerebral cortex nerve injury,[23] as well as Bouchama A et al used whole genome transcriptomics to reveal the molecular signature of HS in humans.[24] However, the use of transcriptomics to explore the molecular mechanisms of HS-induced myocardial injury has not yet been reported.

Therefore, in this study, we investigated the transcriptional profiles of rat myocardial tissue and H9C2 cells after heat stress to explore the pathophysiological mechanisms and to search for key pathogenic genes, which were validated in subsequent experiments.

Materials and Methods

Animals

Sprague-Dawley male rats (220±20 g) were purchased from the Laboratory Animal Center of Xinjiang Medical University. Animal experiments were approved by by the Ethics Committee of the First Affiliated Hospital of Xinjiang Medical University (NO. IACUC-A2312-37) in accordance with the National Institute of Health's guidelines for the care and use of laboratory animals. All rats were housed in an ambient temperature of 25±1°C (humidity: 50±5%), with free access to food and water and a 12-hour light-dark cycle.

Cell Culture and Treatment

Rat H9C2 cell line was purchased from Procell (CL-0089, Wuhan, China) and cultured in high glucose DMEM (Solarbio, Beijing, China) supplied with 10% fetal bovine serum (Gibco, USA) 1% penicillin/ streptomycin (Solarbio) at 37°C in a humidified incubator with 5% CO2. Before heat stress, Jun inhibitor SR11302 (2μm, MCE, HY-15870) was pretreated for 2 hours, and then placed in a carbon dioxide incubator heated to 43°C for heat stress for 4 hours.

Heat Stroke Model

HS was induced by heat exposure in an artificial climate chamber with a temperature of 39.5±0.1°C and a humidity of 60% until the rectal temperature of the rats reached 42.5 ±0.2°C, accompanied by cyanosis of the limbs, cyanosis of the lips and loss of movement. The HS cell model was constructed by placing H9C2 cells in a carbon dioxide incubator at 43 ° C for 4 hours, followed immediately by other experiments.

Echocardiography

Anaesthesia was induced in rats with 5% isoflurane and maintained by mask inhalation with 2% isoflurane for transthoracic echocardiography (Vevo 3100, VisualSonics). The systolic and diastolic dimensions of the rat left ventricle in the long-axis and short-axis M-mode were measured using VevoLAB 3.1.0 software, and the left ventricular ejection fraction (LVEF%) and left ventricular fraction shortening (LVFS%) were calculated. Measurements were obtained on 3 or more consecutive cardiac cycles and averaged for each rat.

Enzyme-Linked Immunosorbent Assay (ELISA)

The concentration of cardiac troponin T (cTNT, A-R01100A, Jiangsu Jingmei Biotechnology Co., Ltd), lactate dehydrogenase (LDH, A-R00574A, Jiangsu Jingmei Biotechnology Co., Ltd), creatine kinase isoenzymes (CK-MB, A-R00592A, Jiangsu Jingmei Biotechnology Co., Ltd), brain natriuretic peptide (BNP, A-R02353A, Jiangsu Jingmei Biotechnology Co., Ltd), tumor necrosis factor (TNF)-α (A-R00166A, Jiangsu Jingmei Biotechnology Co., Ltd), Interleukin (IL) 1β (A-R00040A, Jiangsu Jingmei Biotechnology Co., Ltd), and IL-6 (A-R00175A, Jiangsu Jingmei Biotechnology Co., Ltd) in rat serum were quantified by ELISA kits following the manufacturer's instructions.

Hematoxylin and Eosin (H&E) Staining

To observe the histological changes of LV myocardium, rat LV tissues were fixed with 4% paraformaldehyde for 24 h, embedded in paraffin and cut into 4 μm. Paraffin sections were stained with H&E according to the manufacturer's instructions. After sealing the sections, they were scanned with a digital section scanner (KF-PRO-002).

Transmission Electron Microscopy

Changes in mitochondrial structure of myocardial tissue observed by transmission electron microscopy (TEM) (HI7700, Hitachi, Tokyo, Japan). Rat LV tissues were taken and quickly placed in 2.5% glutaraldehyde solution at 4°C overnight. Afterwards, the samples were fixed with 1% osmium tetroxide for 1h, and then the samples were dehydrated and disposed with different concentrations of ethanol and embedded in epoxy resin. They were then cut into ultra-thin slices and observed using a TEM.

Transcriptome Sequencing

Left ventricular tissue used for transcriptome sequencing analysis was obtained from HS and control rats, and cells were harvested from 4-hour heat stress-treated cells and control cells. Total RNA was extracted from the tissue and H9C2 cells using MJZol total RNA extraction kit (Majorbio, Shanghai, China) according the manufacturer's instructions. RNA purification, reverse transcription, library construction and sequencing were performed at Shanghai Majorbio Bio-pharm Biotechnology Co., Ltd. (Shanghai, China). Sequencing results were analysed using a platform provided by Shanghai Majorbio Bio-pharm Biotechnology.

Identification of Target Genes

We used STRING online tool (https://cn.string-db.org/) for protein-protein interaction analysis and subsequently used Cytoscape software to identify target genes using four different algorithms (Degree, EPC, MCC and MNC). In addition, we further screened target genes using machine learning algorithms including Random Forest (RF) and least absolute shrinkage and selection operator (LASSO).

Quantitative Real-Time PCR

Total RNA from H9C2 cells was individually extracted using TransZol Up Plus RNA Kit (TransGen Biotech, ER501-01-V2). The TRIzol reagent was used to extract total RNA from rat myocardial tissue. cDNA was synthesized using the ABScript RT Master Mix for qPCR with gDNA Remover(RK20429) reagent. After reverse transcription, the Genious 2X SYBR Fast qPCR Mix(RM21204) reagent and the fluorescence quantitative PCR instrument (Thermo Scientific, USA)

were selected for qPCR detection. Relative expression levels were calculated and normalized to GAPDH gene using the $2^{-\Delta\Delta Ct}$ method.

Immunofluorescence

Fresh LV tissues were fixed and embedded using OCT immediately after collection, snap-frozen in liquid nitrogen and placed at −80°C for backup. The frozen LV tissue blocks were cut into 7 μm sections and rewarmed for 30 min at room temperature. Tissue sections was fixed with 4% paraformaldehyde for 15 min, washed with PBS, permeabilised with 0.5% Triton X-100 in PBS for 15 min and blocked with 10% BSA. The primary antibodies used was anti-JUN (1:400, 24,909-1-AP, Proteintech), which were added and incubated with sections overnight at 4°C. Sections were then stained with the secondary antibody (Goat Anti-Mouse lgG(H+L) and nuclei were stained with DAPI (Beyotime). Pictures were obtained by confocal microscope (Zeiss, Germany).

Analysis of Apoptosis

Tunnel staining was performed in accordance with the manufacturer's directions (PF00009, Proteintech). Briefly, the frozen LV tissue blocks were cut into 7 μm sections and rewarmed for 20 min at room temperature. Tissue sections were fixed using 4% paraformaldehyde solution (in PBS) at room temperature for 30 min. After washing with PBS, the sections were incubated at room temperature for 10 min using Proteinase K solution. The TUNEL reaction reagents were used to label DNA breaks at 37°C. After rinsing with PBS, DAPI staining was performed for 20 min. Confocal microscope (Zeiss, Germany) was used to for image acquisition.

Flow Cytometry

After H9C2 cells were pretreated with or without SR11302 for 2 hours and stimulated with heat stress for 4 hours, cell apoptosis and mitochondrial membrane potential (MMP) was analyzed by using Annexin V PE/7AAD Apoptosis Detection Kit (BD Biosciences, 559763) and Mitochondrial Membrane Potential Assay Kit with JC-1 (Solarbio, M8650) according to the manufacturer's instructions. Flow cytometry analyses were performed on a BD FACSCanto II flow cytometer using flow cytometry (Diva software, BD Biosciences, San Jose, CA). FlowJo software (Tree Star, Ashland, OR) was used to analyze data.

Western Blotting

Proteins were extracted from frozen LV tissues or H9C2 cells using RIPA lysate containing protease inhibitors and protein concentrations were determined using BCA Protein Assay (Thermo Fisher Scientific, China, 23225). Proteins were separated using SDS-PAGE and transferred to PVDF membranes (sigma, Millipore), then the membranes were blocked with milk for 2 hours at room temperature and incubated with primary antibodies overnight at 4°C. The density of Western blotting bands was analyzed utilizing Image J software (version 1.8.0, NIH, Bethesda, USA). The primary antibodies included anti-Jun (1:1000, Proteintech), anti-Bcl2 (1:5000, Proteintech), anti-Bax (1:2000, Proteintech) and anti-C-caspase 3 (1:1000, CST).

Statistical Analysis

All data are presented as the mean±standard deviation (SD). Comparisons between groups were made using Student's *t*-test or one-way ANOVA. GraphPad Prism software (version 9.0.2, San Diego, USA) was used for all statistical analyses. P value<0.05 was considered statistically significant.

Results

HS Induced Cardiac Dysfunction and Systemic Inflammation

By constructing a rat model of HS (Figure 1A), we detected a significant elevation of serum markers of myocardial injury in HS rats (Figure 1B–E), accompanied by an increased secretion of serum proinflammatory factors (Figure 1F–H). Echocardiographic results showed that the cardiac function of HS rats decreased significantly compared with the control

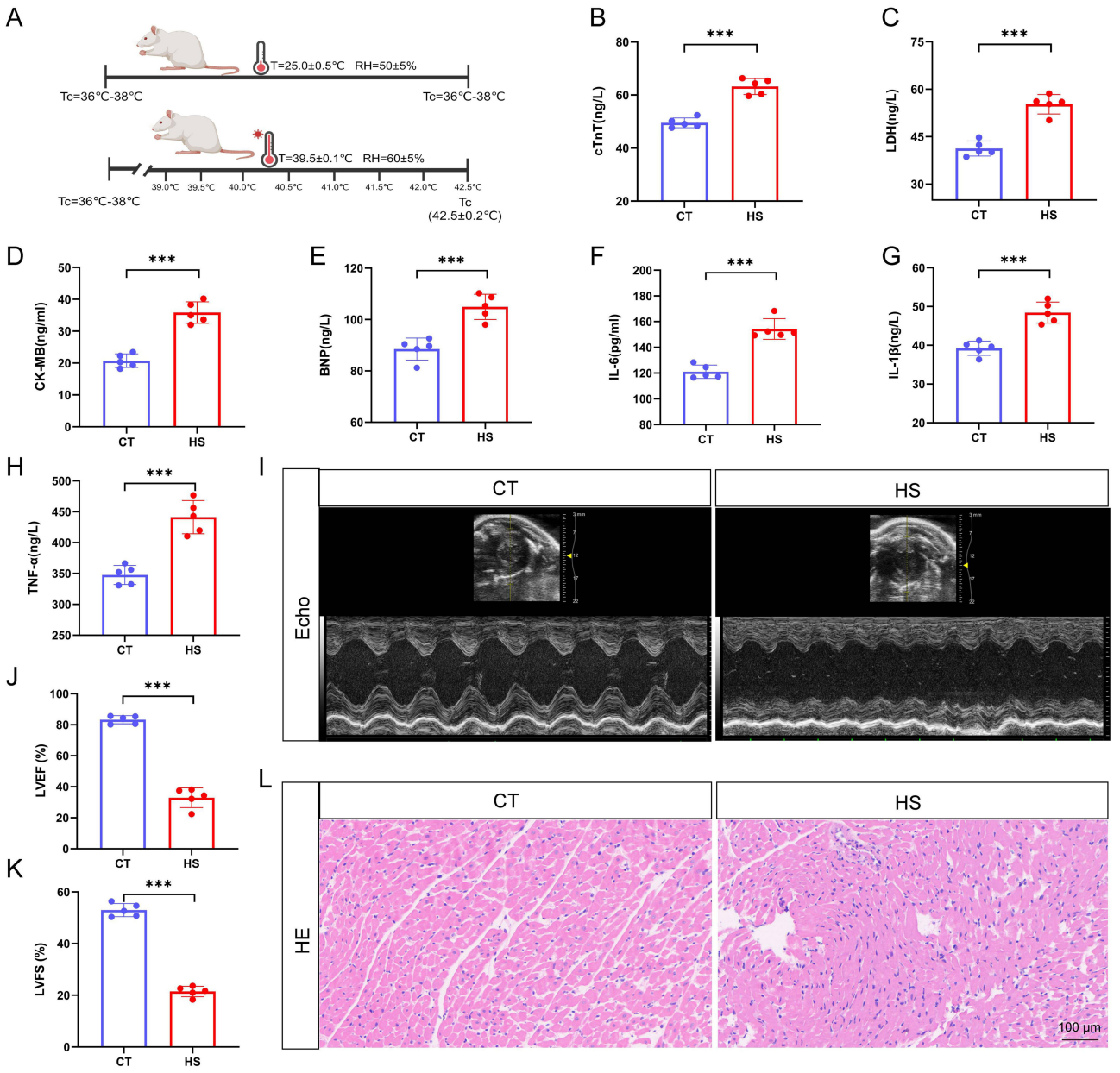

Figure 1 Heat stroke induced severe cardiac dysfunction. (**A**) The schematic diagram of the construction of HS rat model. Created in BioRender. Xiang, J. (2025) https://BioRender.com/7hsbi4b. (**B**–**E**) Serum markers of myocardial injury (cTNT, LDH, CK-MB and BNP) levels in rats. (**F**–**H**) Serum inflammation levels in rats (TNF-α, IL6, and L1β). (**I**) Representative echocardiographic images of HS and control rats. (**J** and **K**) LVEF and LVFS were assessed by echocardiography. (**L**) Representative images of H&E staining. Data are shown as mean±SD. ***P < 0.001.

Abbreviations: CT, control; HS, heat stroke; Tc, core temperature; RH, relative humidity; cTNT, cardiac troponin T; CK-MB, creatine kinase-MB; LDH, lactate dehydrogenase; BNP, brain natriuretic peptide; TNF-α, tumor necrosis factor-α; IL-6, interleukin-6; IL-1β, interleukin-1β; Echo, echocardiography; LVEF, left ventricle ejection fraction; LVFS, left ventricle fractional shortening; H&E, hematoxylin-eosin.

group (Figure 1I–K). H&E staining showed that the myocardium of HS rats was structurally disorganised, irregularly arranged, with blurred transverse lines and unclear borders, accompanied by a large number of inflammatory cells infiltrating (Figure 1L). These results indicated that HS caused serious myocardial injury and inflammation.

Transcriptomic Analysis

To elucidate the potential causes of HS-induced myocardial injury, we performed transcriptomic analysis of rat left ventricular tissue and H9C2 cells. Figure 2A represents the process of constructing the H9C2 cell HS model. Transcriptomics results showed significant differences in gene expression between HS rats and rats in the normal

https://doi.org/10.2147/JIR.S517319

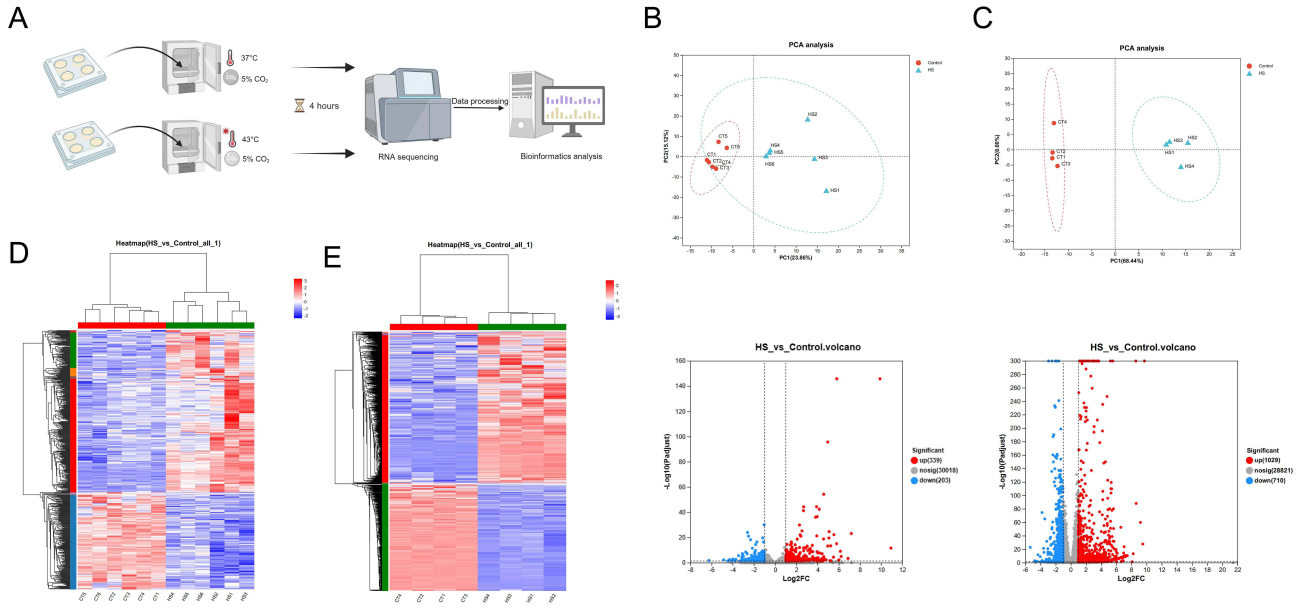

Figure 2 Identification of DEGs. (**A**) Flowchart of H9C2 cell processing. Created in BioRender. Xiang, J. (2025) https://BioRender.com/xoqi3a5. (**B** and **C**) PCA and volcano plot of myocardial tissue (n=6) and H9C2 cell (n=4) transcriptomics. (**D** and **E**) Heatmap of myocardial tissue and H9C2 cell transcriptomics.
Abbreviations: DEGs, differentially expressed genes; PCA, principal component analysis.

group, with a total of 542 differentially expressed genes (DEGs) screened (Padjust<0.05, |Log2FC|>2), of which 339 were up-regulated and 203 were down-regulated (Figure 2B and Supplementary Table 1). Similarly, H9C2 cell transcriptomics results showed significant differences in gene expression between the two, with a total of 1739 DEGs screened (Padjust<0.05, |Log2FC|>2), including 1029 up-regulated genes and 710 down-regulated genes (Figure 2C and Supplementary Table 2). Figure 2D and E represented the heat maps of DEGs in rat tissue and H9C2 cells, respectively. The above results indicated that HS affected gene expression in both tissues and cells.

HS Induced Tissue and Cellular Injury Mainly by Regulating Apoptosis

In order to further elucidate the pathological mechanism, we performed functional enrichment analysis of two groups of DEGs. Analysis of gene ontology (GO) enrichment of tissue DEGs showed that DEGs were mainly enriched in biological processes such as regulation of programmed cell death and apoptosis, and analysis of Kyoto Encyclopedia of Genes and Genomes (KEGG) pathway enrichment of DEGs showed that DEGs were mainly enriched in "TNF signaling pathway", "MAPK signaling pathway" and "PI3K-Akt pathway" pathways (Figure 3A and Supplementary Table 3). Similarly, GO enrichment analysis of cellular DEGs showed that DEGs were mainly enriched in the regulation of programmed cell death and apoptosis, while KEGG results showed that DEGs were mainly enriched in pathways such as "IL-17 signaling pathway"(Figure 3B and Supplementary Table 4). Gene set enrichment analysis (GSEA) analysis was performed for all genes, and Figure 3C and D represented the GSEA results for HS rat myocardium and H9C2 cells, respectively, suggesting that myocardial injury was significantly associated with apoptosis and mitochondria (|NES|>1, Padjust<0.05, Supplementary Tables 5 and 6). In addition, we took intersections of tissue and cellular DEGs for joint analysis (Figure 3E). The results showed that Jun exists as a key gene in all DEGs (Figure 3F). Similarly, GO analyses showed that these common DEGs are involved in biological processes such as apoptosis regulation, response to temperature stimuli and regulation of inflammatory responses (Figure 3G). The above results suggested that apoptosis plays a pivotal role in HS-induced myocardial and cellular injury.

HS Induced Mitochondrial Apoptosis in Tissues and Cells

Mitochondrial apoptosis, a major pathway of apoptosis, plays an important role in various myocardial injuries, and enrichment of biological processes such as mitochondria and apoptosis was observed in GSEA enrichment analysis.

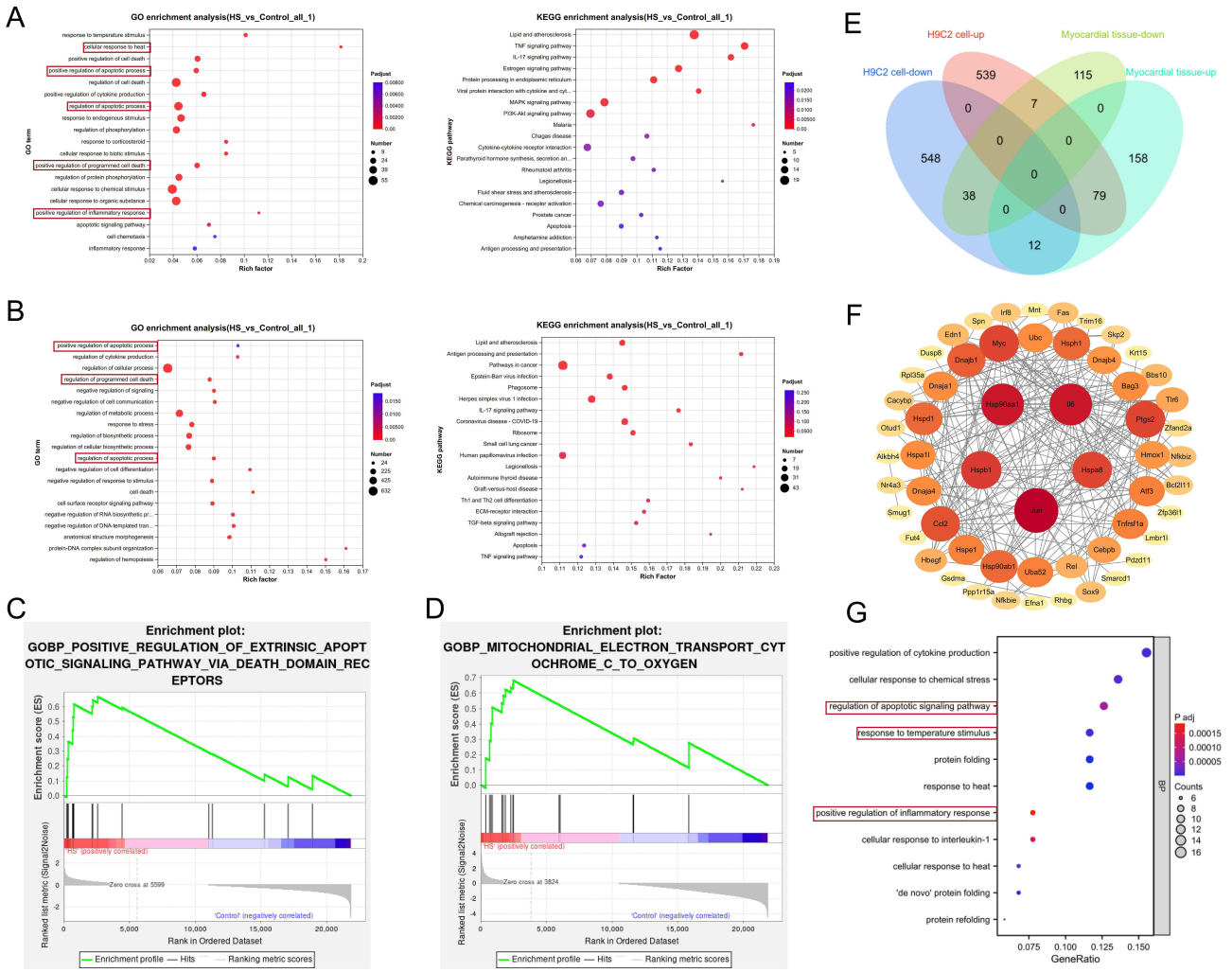

Figure 3 Functional enrichment analysis of DEGs. (**A**) GO and KEGG analysis of myocardial tissue transcriptomics. (**B**) GO and KEGG analysis of H9C2 cell transcriptomics. (**C** and **D**) GSEA analysis of myocardial tissue and H9C2 cell transcriptomics, respectively. (**E**) Identification of common DEGs in myocardial tissue and H9C2 cells. (**F**) Protein-protein interaction analysis of common DEGs. (**G**) GO analysis of common DEGs in myocardial tissue and H9C2 cell transcriptomics.
Abbreviations: GO, gene ontology; KEGG, Kyoto Encyclopedia of Genes and Genomes; DEGs, differentially expressed genes; BP, biological process; GSEA, gene set enrichment analysis.

Therefore, we performed further analyses of mitochondria-related genes. GSEA analysis of mitochondria-related genes in myocardial tissue transcriptomics showed that these genes were significantly enriched for the regulation of apoptotic signaling pathways and in response to temperature stimuli (Figure 4A and B, Supplementary Table 7, |NES|>1, Padjust<0.05). Figure 4C and D showed differentially expressed mitochondrial-related genes in tissues and H9C2 cells using cyclic heatmaps, respectively. Figure 4E and F showed the terms/pathways corresponding to differentially expressed mitochondria-related genes using enriched chordal plots, respectively. Meanwhile, our functional enrichment analysis of these differentially expressed mitochondria-related genes revealed that these genes were significantly enriched in apoptosis-related pathways (Figure 4G and H; Supplementary Tables 8 and 9). The above findings confirmed that HS-induced myocardial and cellular injury was mainly achieved through mitochondrial apoptosis.

Jun Was the Key Target Gene in HS-Induced Myocardial Apoptosis

Having clarified that apoptosis was the primary phenotype of HS-induced myocardial injury, we next screened DEGs in apoptosis-related biological processes and pathways to target key target genes. Figure 5A and B demonstrated the distribution of DEGs on the apoptotic pathway. Figure 5C and D represented the relative expression of apoptosis-related DEGs in tissues and cells as measured by transcripts per million reads (TPM) values, respectively. Figure 5E showed

https://doi.org/10.2147/JIR.S517319

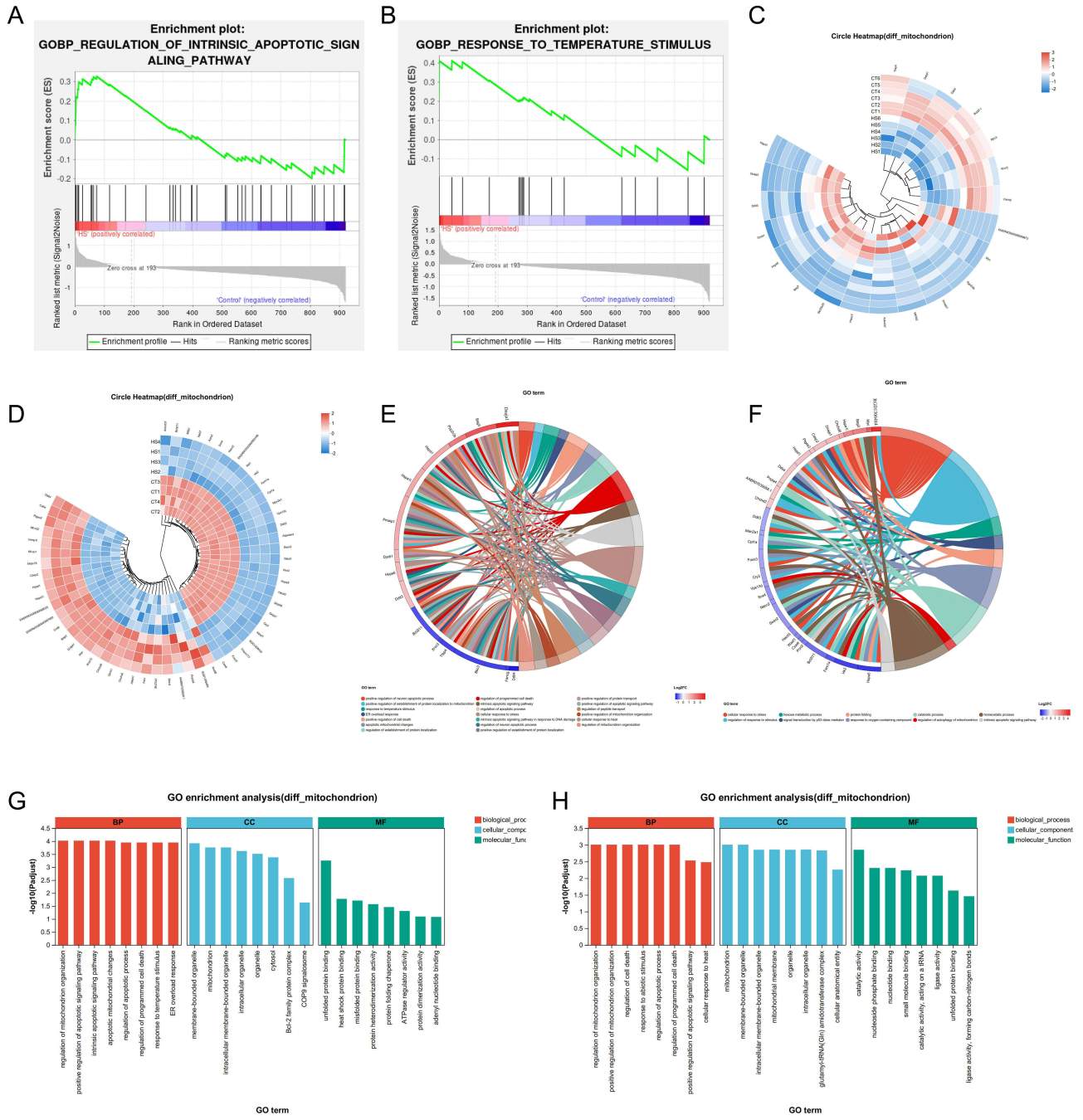

Figure 4 Functional enrichment analysis of mitochondria-related genes. (**A** and **B**) GSEA analysis of mitochondria-related genes in myocardial tissue transcriptomics. (**C** and **D**) Cyclic heatmap of differential expression of mitochondria-related genes in myocardial tissue and H9C2 cell transcriptomics. (**E** and **F**) Enriched chordal plots of pathways corresponding to differential expression of mitochondria-related genes in myocardial tissue and H9C2 cell transcriptomics. (**G** and **H**) GO analysis of differential expression of mitochondria-related genes in myocardial tissue and H9C2 cell transcriptomics.
Abbreviations: GO, gene ontology; GSEA, gene set enrichment analysis; BP, biological process; CC, cellular component; MF, molecular function.

protein-protein interaction network analysis of all apoptosis-related DEGs using STRING. Figure 5F–I represented the top 5 apoptosis-related DEGs screened using different algorithms for apoptosis-related DEGs using Cytoscape software. Jun showed consistent trends in tissue and cellular expression and was at the top of the different algorithms, including being central to all DEGs (Figure 3F). Figure 6A and B represented the use of the Random Forest algorithm to demonstrate the importance of apoptosis-related DEGs in tissues and cells (Supplementary Table 10). Figure 6C–F showed the feature screening of apoptosis-related DEGs in tissues and cells, respectively, using the LASSO algorithm

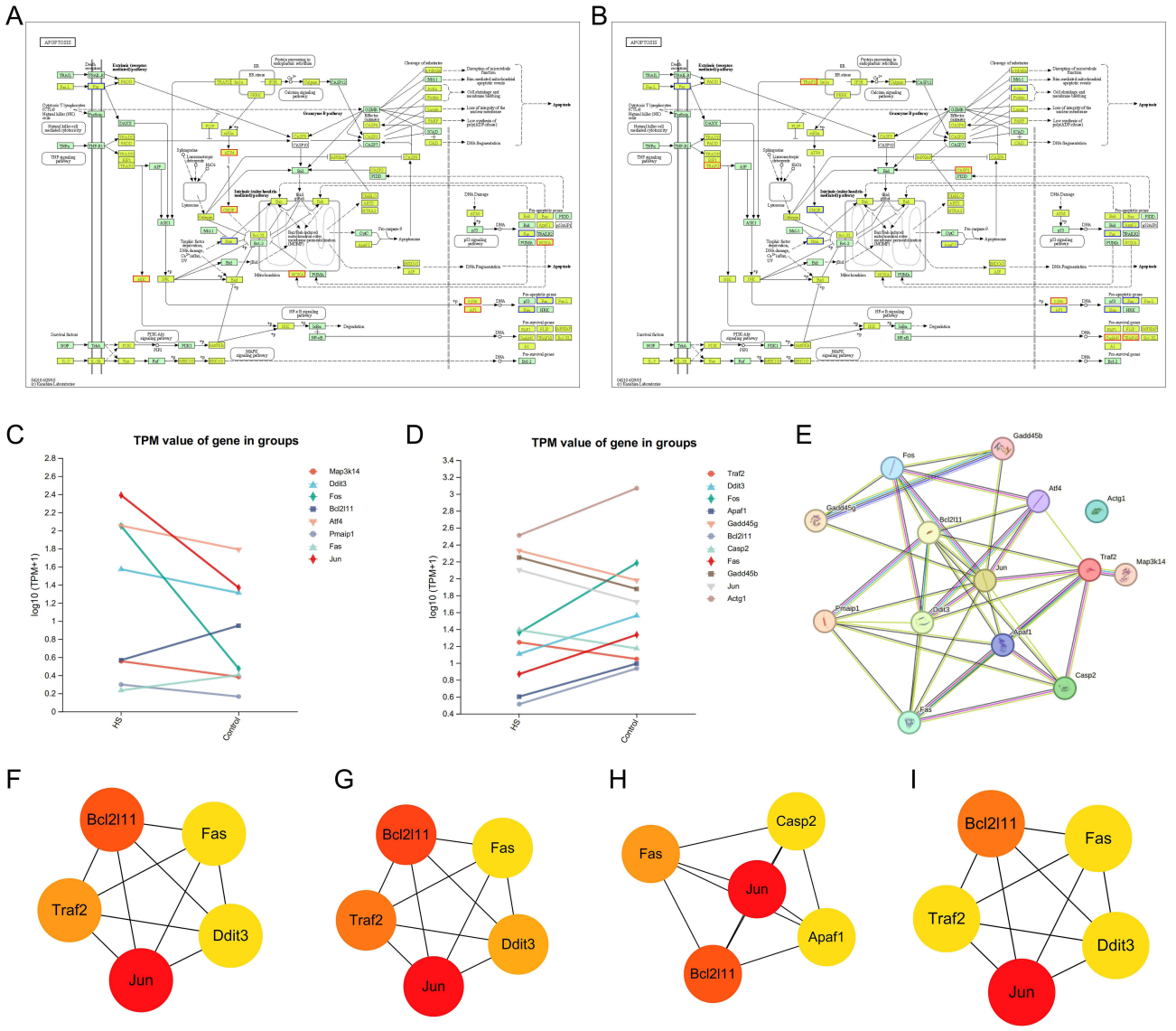

Figure 5 Identification of differentially expressed apoptosis-related genes. (**A** and **B**) Distribution of DEGs on the apoptotic pathway in myocardial tissue and H9C2 cell transcriptomics. (**C** and **D**) Relative expression of apoptosis-related DEGs in myocardial tissue and H9C2 cell transcriptomics. (**E**) Protein-protein interaction analysis of differentially expressed mitochondria-related genes. (**F–I**) The top 5 apoptosis-related DEGs screened with different algorithms (Degree, EPC, MCC and MNC) using Cytoscape software.

Abbreviations: DEGs, differentially expressed genes; TPM, transcripts per million.

(Supplementary Table 11). By taking the intersection of key genes from tissues and cells identified by different methods, we obtained key target genes (Figure 6G). Thus, Jun was considered as a target for our interventions and therapies.

Jun Expression Was Up-Regulated in HS Rat Myocardium with Disruption of Mitochondrial Structure and Increased Apoptosis

To further validate the transcriptomics sequencing results, we used qRT-PCR, Western blotting and immunofluorescence experiments to confirm that Jun expression was up-regulated in HS rats compared to the control group (Figure 7A–E). Meanwhile, transmission electron microscopy results showed that HS resulted in severe disruption of the mitochondrial structure, which was mainly characterized by mitochondrial swelling and mitochondrial cristae disruption (Figure 7F). Finally, the results of our Western blotting and immunofluorescence experiments showed a significant increase in apoptosis in HS rat myocardial tissue (Figure 7G–L). The above experimental results further confirmed that up-

https://doi.org/10.2147/JIR.S517319

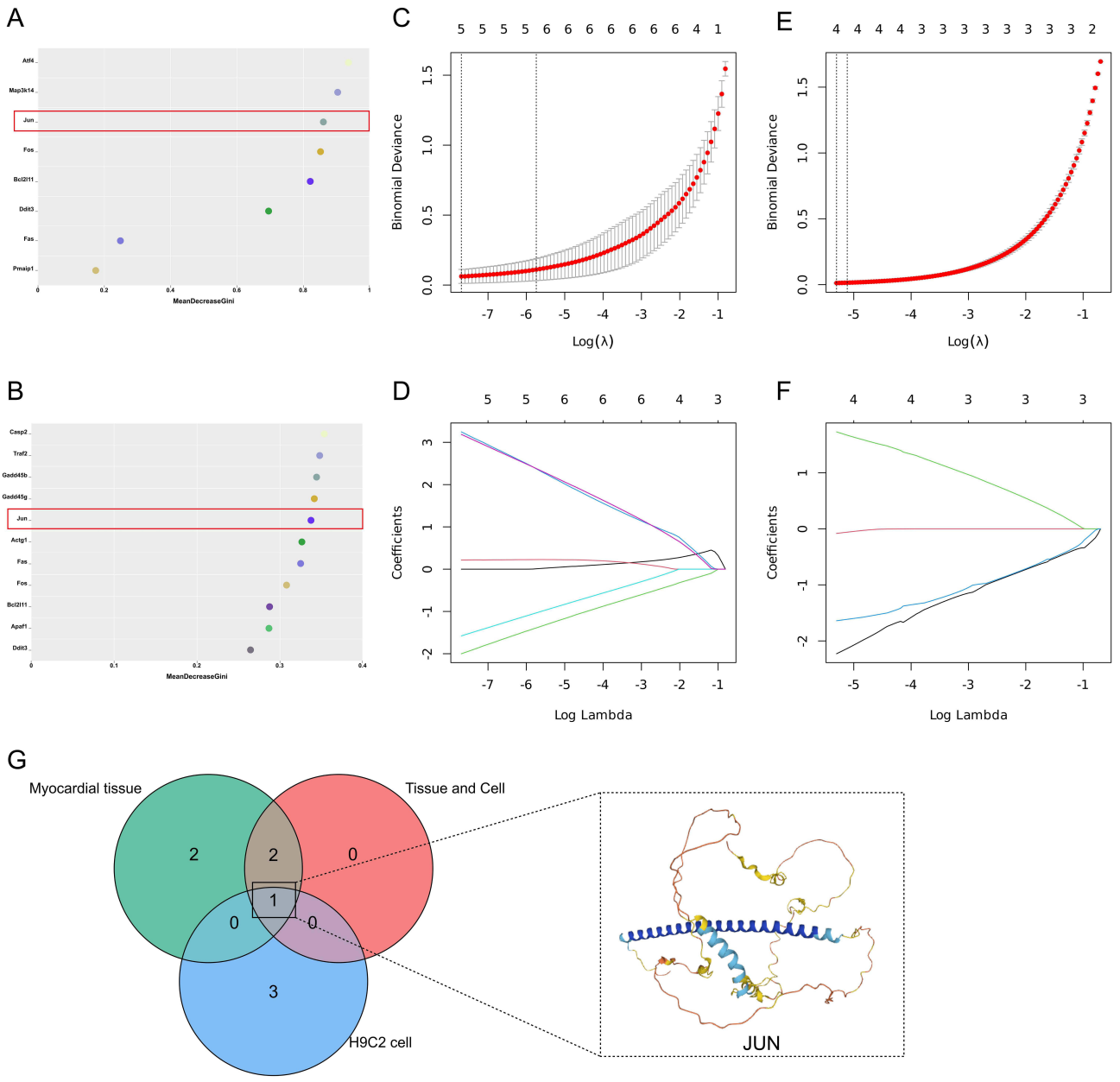

Figure 6 Identification of the key target genes. (**A** and **B**) Results of the RF algorithm for apoptosis-related DEGs in myocardial tissue and H9C2 cell transcriptomics. (**C** and **D**) LASSO analysis with standard lambda in myocardial tissue transcriptomics. (**E** and **F**) LASSO analysis with standard lambda in H9C2 cell transcriptomics. (**G**) The results of different algorithms were taken to intersect to screen for key genes.
Abbreviations: DEGs, differentially expressed genes; RF, random forest; LASSO, least absolute shrinkage and selection operator.

regulation of Jun protein expression, disruption of mitochondrial structure and increased apoptosis in rat myocardial tissues were indeed involved in HS-induced myocardial injury.

Inhibition of Jun Expression Improves Mitochondrial Membrane Potential and Attenuates Cell Apoptosis

Next, we further verified whether Jun expression affected mitochondrial alterations and cell apoptosis at the cellular level. Figure 8A represented the schematic diagram of H9C2 cell processing. The results showed that the use of Jun inhibitor (SR11302) reduced heat stress-induced high expression of Jun mRNA and protein compared with the HS group (Figure 8B–D). Flow cytometry results showed that the Jun inhibitor (SR11302) significantly improved mitochondrial

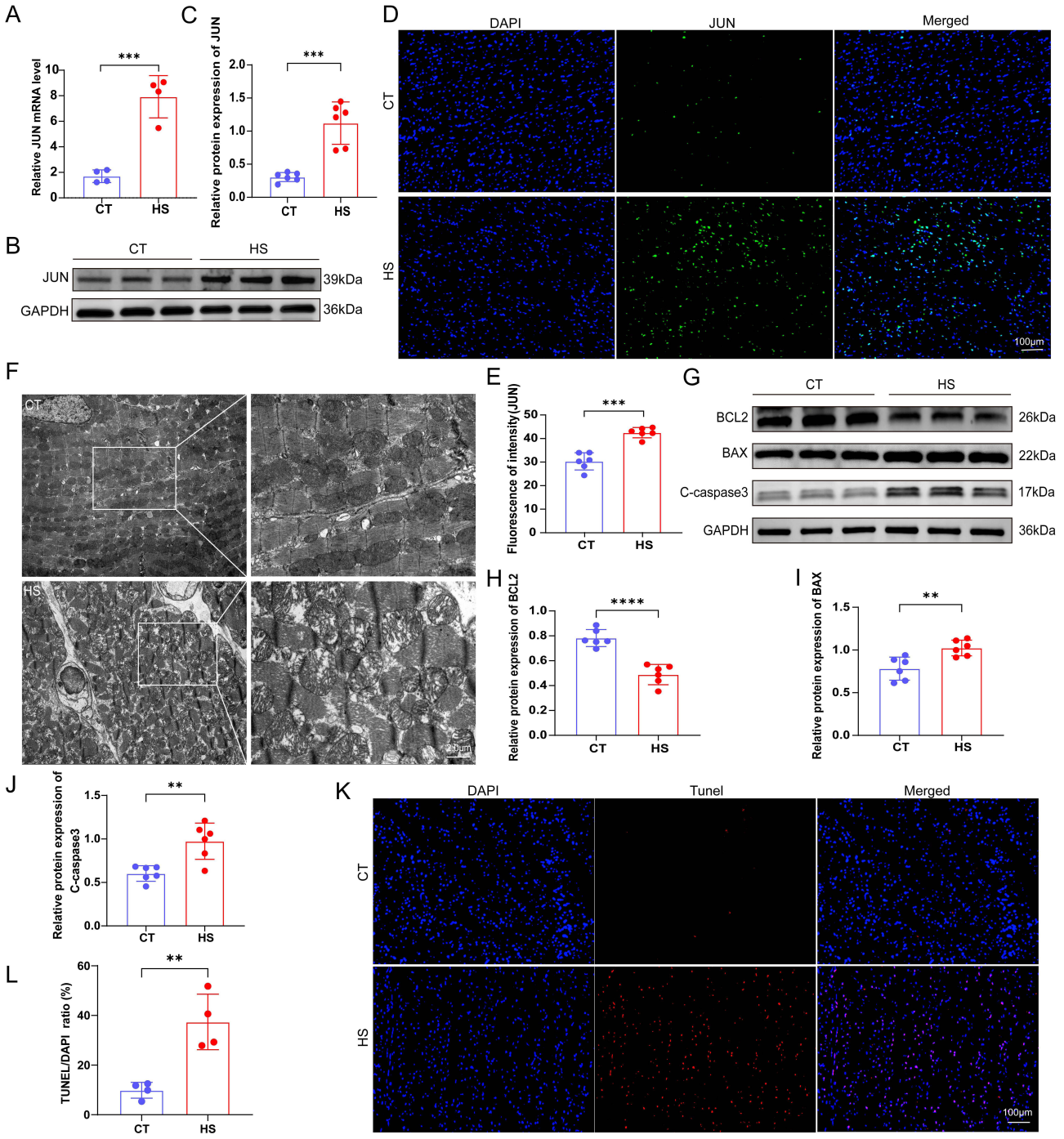

Figure 7 Jun expression was upregulated in HS rat myocardial tissues, with disruption of mitochondrial structure and increased apoptosis. (**A**) The relative mRNA levels of Jun in rat myocardial tissue was measured by the qRT-PCR(n=4). (**B** and **C**) Western blotting results of Jun in rat myocardial tissues and statistical analysis (n=6). (**D** and **E**) Immunofluorescence was used to assess the expression of Jun in rat myocardial tissues. (**F**) Representative mitochondrial TEM images of the HS and CT groups. (**G–J**) Western blotting results of BCL2, BAX, and C-caspase3 in rat myocardial tissues and statistical analysis (n=6). (**K** and **L**) TUNEL assay of rat hearts and its statistical analysis (n=4). Data are shown as mean±SD. **P < 0.01, ***P < 0.001, ****P < 0.0001.

Abbreviations: TEM, transmission electron microscopy; qRT-PCR, Quantitative reverse transcription polymerase chain reaction; BCL2, B-cell lymphoma-2; BAX, Bcl-2 Associated X protein; C-caspase 3, Cleaved-caspase3.

membrane potential compared with the HS group (Figure 8E and F). Meanwhile, it was confirmed by Western blotting and flow cytometry experiments that Jun inhibitor (SR11302) significantly alleviated apoptosis caused by heat stress (Figure 8G–L). The above cellular experiments suggest that Jun-mediated mitochondrial apoptosis is involved in HS-induced myocardial injury. However, its specific mechanism still needs to be further explored.

https://doi.org/10.2147/JIR.S517319

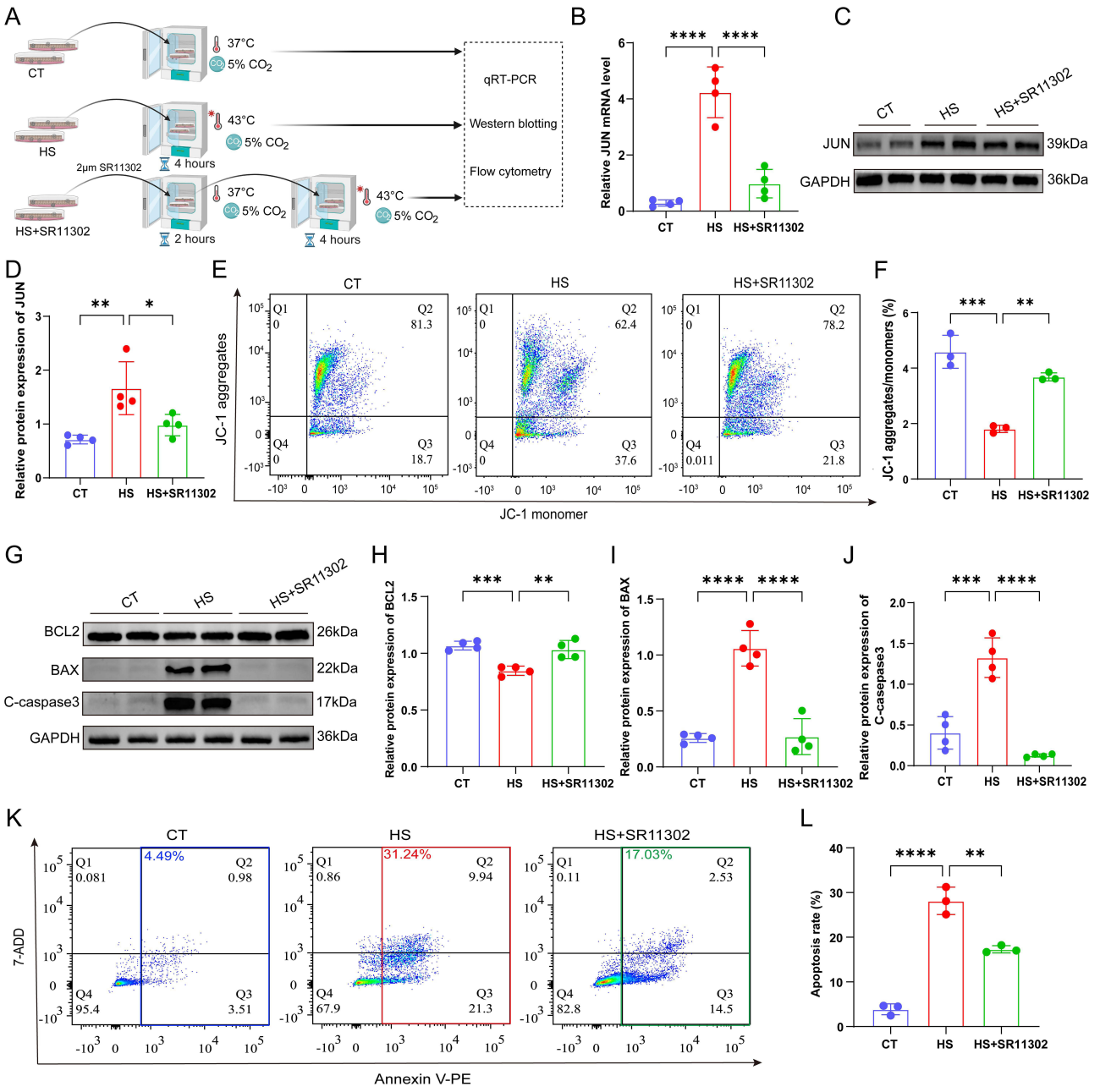

Figure 8 Jun inhibitor (SR11302) ameliorated mitochondrial membrane potential and attenuated apoptosis in H9C2 cells. (**A**) Schematic diagram of H9C2 cell treatment. Created in BioRender. Xiang, J. (2025) https://BioRender.com/5ycomjj. (**B**) The relative mRNA levels of Jun in H9C2 cells was measured by the qRT-PCR(n=4). (**C** and **D**) Western blotting results of Jun in H9C2 cells and statistical analysis (n=4). (**E** and **F**) SR11302 improved mitochondrial membrane potential as evidenced by flow cytometry in H9C2 cells (n=3). (**G**–**J**) Western blotting results of BCL2, BAX, and C-caspase3 in H9C2 cells and statistical analysis (n=4). (**K** and **L**) H9C2 cardiomyocyte apoptosis determined by flow cytometry (n=3). Data are shown as mean±SD. **P < 0.01, ***P < 0.001, ****P < 0.0001.

Abbreviations: qRT-PCR, Quantitative reverse transcription polymerase chain reaction; BCL2, B-cell lymphoma-2; BAX, Bcl-2 Associated X protein; C-caspase 3, Cleaved-caspase3.

Discussion

HS-induced organ injury involves multiple factors in an extremely complex biochemical cascade, and the cardiovascular system is undoubtedly considered to be the first to be mobilised during HS. Also as a heat-sensitive organ, it is one of the most vulnerable organs during HS.[7,8] However, the exact mechanism of HS induced myocardial injury is still unclear, and there is a lack of effective prevention and treatment of cardiovascular diseases at high temperatures. In the present study, by constructing a rat model of HS, we observed that HS rats exhibited systemic inflammatory responses,

myocardial injury and a significant decrease in cardiac function. To further clarify the mechanism of myocardial injury in HS rats, we simultaneously constructed a cellular heat stress model using the H9C2 cell line, and found that inflammatory response, mitochondrial dysfunction, and apoptosis were the main biological processes involved through combined tissue and cellular transcriptomics analysis. Additionally, in order to find targets for HS-induced myocardial injury prevention and treatment, we further mined the DEGs and found that Jun-mediated apoptosis plays a dominant role in myocardial injury. And the above conclusion was further confirmed in subsequent animal and cellular experiments.

Mitochondria constitute more than 35% of cardiomyocyte volume and are the main source of energy for cardiomyocytes, making cardiomyocyte mitochondria critical to cardiac function.[25] Under physiological conditions, mitochondria perform a variety of functions dependent on their own structural integrity. Previous studies have shown that significant changes in myocardial mitochondrial structure and function in heat-exposed rats are an important mechanism leading to cardiomyocyte injury.[19] Significant impairment of mitochondrial morphology and function in H9C2 cells under heat stress conditions was also observed in the study of Chen et al.[18] Furthermore, Zhang et al demonstrated that higher Hsp90 levels significantly reversed HS-induced myocardial mitochondrial injury by activating Akt-Bcl-2 and PKM2-Bcl -2 signalling pathways.[26] Consistent with previous findings, our transcriptomics revealed that HS induced significant alterations in myocardial mitochondria-associated proteins, and transmission electron microscopy results indicated that HS resulted in alterations such as mitochondrial swelling and cristae rupture. These results further confirm that mitochondria is one of the main organelles of heat injury, and targeting mitochondria is a promising means to prevent HS-induced myocardial injury.

HS has multiple toxic effects on cardiomyocytes, including apoptosis.[6] Apoptosis, also known as programmed cell death, plays an important role in maintaining tissue homeostasis. It is triggered by extrinsic apoptotic pathways, intrinsic apoptotic pathways and endoplasmic reticulum stress-related apoptotic pathways, among which intrinsic apoptotic pathway is mainly mediated by mitochondria.[27,28] Apoptosis has been extensively studied in cardiomyocytes, including HS-induced cardiomyocyte injury. Studies have reported that heat stress induced myocardial injury and apoptosis in mice by activating endoplasmic reticulum stress (ERS).[29] Chen et al demonstrated that the expression of GRP78 and CHOP was significantly elevated after HS, whereas the expression of Bcl2 was significantly reduced, confirming that HS triggered ERS-mediated apoptosis.[30] And additional curcumin supplementation was able to reverse the above changes and protect the myocardium from HS-induced ERS-mediated apoptosis. Qian et al showed that HS induced apoptosis and necrosis of cardiomyocytes in a time- and dose-dependent manner.[19] In vivo studies also revealed that HS induced alterations in mitochondrial membrane permeability transition leading to caspase-3 activation, whereas transfection with Bcl2 resulted in Bcl2 overexpression in cardiomyocytes, which protected the mitochondria and reduced HS-induced cardiomyocyte injury.[19] In addition to apoptosis, it has been shown that inhibition of TLR4 attenuates HS-induced cardiomyocyte injury.[18] This study is the first to demonstrate that HS can activate an TLR4/NF-κB-induced ferroptosis. Inhibiting the TLR4/NF-κB pathway can improve H9C2 cell viability and suppresses the inflammatory level and ferroptosis.[18] Thus, TLR4 could be an effective target for intervention in HS-induced myocardial injury. Our transcriptomic sequencing suggested that HS-induced myocardial injury mainly involves apoptotic biological processes, which was further validated in animal and cellular models using Western blotting, tunnel staining and flow cytometry. Thus, previous studies and our results further suggest that mitochondria-mediated apoptosis plays an important role in HS-induced myocardial injury.

Currently, the main reason why there are no preventive and therapeutic strategies for myocardial injury during HS is the lack of targets to treat the disease. Therefore, researchers have been working on the target of HS induced myocardial injury. For example, TLR4,[18] Bcl2,[19] and Hsp90.[26] Through transcriptomic data, we are also trying to find new targets of HS induced myocardial injury. Analysis using the String online tool and Cytoscape software revealed that Jun was dominant in all DEGs, highly expressed in HS and enriched in the apoptotic pathway. Subsequently, we confirmed a significant increase of Jun protein in myocardial tissue of HS rats. In cell experiments, our results showed that HS leads to a significant increase in Jun protein expression in H9C2 cells, and the use of Jun protein inhibitors (SR11302) can significantly improve mitochondrial morphology and reduce apoptosis. These evidences suggest that Jun-mediated mitochondrial damage leading to apoptosis may play a critical role in HS-induced myocardial injury, and Jun may be a new key target for the prevention and treatment of HS-induced myocardial injury.

Jun gene, encoding c-Jun protein, is a transcription factor of the AP-1 family, which is not only the target of many extracellular stimuli, but plays an important role in mediating cellular responses.[31,32] In response to environmental stresses, such as pro-inflammatory factors, ultraviolet, ischaemia and hypoxia, c-Jun expression is significantly elevated and is involved in various cellular activities such as proliferation, apoptosis and tissue morphogenesis.[32,33] However, evidence from published studies suggesting a precise role for c-Jun in cell proliferation and apoptosis is still controversial. It has been shown that under hypoxic conditions, c-Jun protects H9C2 cells from apoptosis through the PTEN/Akt signalling pathway and promotes the survival of H9C2 cells.[31] In cancer cells, c-Jun has also been reported to protect cells from apoptosis by inhibiting the pro-apoptotic effects of p53.[34] Nonetheless, studies have also shown that c-Jun can promote apoptosis by increasing the expression of pro-apoptotic genes such as Bim.[35] Furthermore, there is evidence that the pro- or anti-apoptotic effect of c-Jun manifested depends on the level of mitochondrial damage, whereby the response of c-Jun signaling to different levels of mitochondrial stress, thus appropriately mediating apoptosis or cell protection.[36] And our findings seem to be more supportive of the existence of c-Jun as a pro-apoptotic factor. However, most of these studies, including the present study, were limited to describing the correlation between c-Jun and apoptosis and did not further investigate its potential roles and mechanisms. Therefore, after targeting the key genes, our research group is actively constructing Jun gene knockout mice for more in-depth study of its exact mechanism in HS-induced cardiomyocyte apoptosis. Based on our experimental findings and existing literature, we propose the following potential pathways of Jun regulating mitochondrial apoptosis. Activation of Jun leads to its dimerization with other transcription factors (eg c-Fos) to form the AP-1 complex. The complex binds directly to pro-apoptotic gene promoters (eg, Bim, Bax) or represses anti-apoptotic genes (eg, Bcl-2), thereby regulating mitochondrial outer membrane permeability (MOMP) and cytochrome C release.[37] Jun could synergize with p53 to amplify apoptotic signals. For instance, p53-mediated suppression of Bcl-2 might lower the threshold for c-Jun-dependent activation of pro-apoptotic effectors.[38] Additionally, c-Jun may integrate stress signals from the endoplasmic reticulum (eg, calcium overload) to coordinate mitochondrial apoptosis.[39] Furthermore, the interaction between heat shock proteins and Jun may be one of its mechanisms. For example, the JNK/c-Jun pathway interacts with HSP70,[40] and the potential synergistic effect between Jun/AP-1 and HSF1.[41] However, the exact mechanism remains unknown and needs to be studied in depth in the future.

Limitations

Although the present study provides a potential therapeutic target for elucidating HS-induced myocardial injury, it has some limitations. First of all, knockdown or suppression of Jun at the animal gene level was not performed in this study, which is what our group will do in the future. Second, The specific pathways by which Jun regulates mitochondrial apoptosis are unknown and need to be explored in more in-depth studies in the future. Finally, other key genes screened in this study deserve further investigation in HS-induced myocardial injury.

Conclusion

In conclusion, the present study demonstrated that Jun-mediated mitochondrial damage leading to cardiomyocyte apoptosis was involved in HS-induced myocardial injury by transcriptomic sequencing combined with experiments. Jun may represent a promising preventive and therapeutic target for HS-induced myocardial injury.

Abbreviations

HS, heat stroke; TNF-α, tumour necrosis factor-alpha; IL-1β, interleukin-1β; IL-6, interleukin-6; ELISA, enzyme-linked immunosorbent assay; cTNT, cardiac troponin T; LDH, lactate dehydrogenase; CK-MB, creatine kinase isoenzymes; BNP, brain natriuretic peptide; LVEF, left ventricular ejection fraction; LVFS, left ventricular fraction shortening; RF, Random Forest; LASSO, least absolute shrinkage and selection operator; MMP, mitochondrial membrane potential; DEG, differentially expressed genes; GO, gene ontology; KEGG, Kyoto Encyclopedia of Genes and Genomes; GSEA, Gene set enrichment analysis; TPM, transcripts per million.

Data Sharing Statement

All other data in this article are available from the corresponding author upon reasonable request.

Ethics Approval and Consent to Participate

The study protocol was approved by the Animal Ethics Committee of the First Affiliated Hospital of Xinjiang Medical University, China (Approval NO. IACUC-A2312-37). All studies conformed to the Guide for the Care and Use of Laboratory Animals (National Academies Press, 2011).

Acknowledgments

We are grateful for the sacrifice of laboratory animals in our experiments and for the great sacrifices they make for our scientific research and human health. In addition, we would like to thank BioRender for providing us with a drawing platform.

Funding

This work was supported by the National Natural Science Foundation Of China [grant number 82370326, 82260065, 82200360], the Natural Science Foundation of Xinjiang Uygur Autonomous Region [grant number 2021D01E27, 2022TSYCCX00981].

Disclosure

The authors have declared no competing interests in this work.

References

1. Toutant S, Gosselin P, Bélanger D, Bustinza R, Rivest S. An open source web application for the surveillance and prevention of the impacts on public health of extreme meteorological events: the SUPREME system. *Int J Health Geogr*. 2011;10(1):39. doi:10.1186/1476-072X-10-39
2. Niu B, Zhang T, Hu H, Cao B. Transcriptome sequencing reveals astrocytes as a therapeutic target in heat-stroke. *Neurosci Bull*. 2017;33(6):627–640. doi:10.1007/s12264-017-0156-8
3. Peiris AN, Jaroudi S, Noor R. Heat Stroke. *JAMA*. 2017;318(24):2503. doi:10.1001/jama.2017.18780
4. Leon LR, Bouchama A. Heat stroke. *Compr Physiol*. 2015;5(2):611–647. doi:10.1002/cphy.c140017
5. Crandall CG, González-Alonso J. Cardiovascular function in the heat-stressed human. *Acta Physiol*. 2010;199(4):407–423. doi:10.1111/j.1748-1716.2010.02119.x
6. Xia R, Sun M, Li Y, et al. The pathogenesis and therapeutic strategies of heat stroke-induced myocardial injury. *Front Pharmacol*. 2024;14:1286556. doi:10.3389/fphar.2023.1286556
7. Ko WC, Lin CH, Lee JJ, Chang CP, Chao CM. Therapeutic hypothermia protects against heat stroke-induced arterial hypotension via promoting left ventricular performance in rats. *Int J Med Sci*. 2020;17(4):525–535. doi:10.7150/ijms.39745
8. Low DA, Keller DM, Wingo JE, Brothers RM, Crandall CG. Sympathetic nerve activity and whole body heat stress in humans. *J Appl Physiol*. 2011;111(5):1329–1334. doi:10.1152/japplphysiol.00498.2011
9. Desai Y, Khraishah H, Alahmad B. Heat and the Heart. *Yale J Biol Med*. 2023;96(2):197–203. doi:10.59249/HGAL4894
10. Knochel JP, Beisel WR, Herndon EG, Gerard ES, Barry KG. The renal, cardiovascular, hematologic and serum electrolyte abnormalities of heat stroke. *Am J Med*. 1961;30(2):299–309. doi:10.1016/0002-9343(61)90101-2
11. Roberts GT, Ghebeh H, Chishti MA, et al. Microvascular injury, thrombosis, inflammation, and apoptosis in the pathogenesis of heatstroke: a study in baboon model. *Arterioscler Thromb Vasc Biol*. 2008;28(6):1130–1136. doi:10.1161/ATVBAHA.107.158709
12. Leon LR, Helwig BG. Heat stroke: role of the systemic inflammatory response. *J Appl Physiol*. 2010;109(6):1980–1988. doi:10.1152/japplphysiol.00301.2010
13. Zhang ZT, Gu XL, Zhao X, et al. NLRP3 ablation enhances tolerance in heat stroke pathology by inhibiting IL-1β-mediated neuroinflammation. *J Neuroinflammation*. 2021;18(1):128. doi:10.1186/s12974-021-02179-y
14. Yu M, Wen N, Wenzhong Z, Yuanchang X, Xiaoming D, Yongjin L. Effect of repeated ischaemic preconditioning on TLR4 and proinflammatory cytokines TNF-α and IL-1β in myocardial ischaemia-reperfusion injury in a rat model. *Arch Med Sci*. 2010;6(6):843–847. doi:10.5114/aoms.2010.19289
15. Lin X, Lin CH, Zhao T, et al. Quercetin protects against heat stroke-induced myocardial injury in male rats: antioxidative and antiinflammatory mechanisms. *Chem Biol Interact*. 2017;265:47–54. doi:10.1016/j.cbi.2017.01.006
16. Lin X, Lin CH, Liu R, et al. Myricetin against myocardial injury in rat heat stroke model. *Biomed Pharmacother*. 2020;127:110194. doi:10.1016/j.biopha.2020.110194
17. Chen F, Li H, Zhu G, Chen X, Tang Z. Sodium tanshinone IIA sulfonate improves inflammation, aortic endothelial cell apoptosis, disseminated intravascular coagulation and multiple organ damage in a rat heat stroke model. *Mol Med Rep*. 2017;16(1):87–94. doi:10.3892/mmr.2017.6573
18. Chen D, Geng Y, Deng Z, et al. Inhibition of TLR4 alleviates heat stroke-induced cardiomyocyte injury by down-regulating inflammation and ferroptosis. *Molecules*. 2023;28(5):2297. doi:10.3390/molecules28052297
19. Qian L, Song X, Ren H, Gong J, Cheng S. Mitochondrial mechanism of heat stress-induced injury in rat cardiomyocyte. *Cell Stress Chaperones*. 2004;9(3):281–293. doi:10.1379/csc-20r.1
20. Karczewski KJ, Snyder MP. Integrative omics for health and disease. *Nat Rev Genet*. 2018;19(5):299–310. doi:10.1038/nrg.2018.4
21. Lockhart DJ, Winzeler EA. Genomics, gene expression and DNA arrays. *Nature*. 2000;405(6788):827–836. doi:10.1038/35015701

22. Yang Y, Hao Z, An N, et al. Integrated transcriptomics and metabolomics reveal protective effects on heart of hibernating Daurian ground squirrels. *J Cell Physiol*. 2023;238(11):2724–2748. doi:10.1002/jcp.31123
23. Fang W, Yin B, Fang Z, et al. Heat stroke-induced cerebral cortex nerve injury by mitochondrial dysfunction: a comprehensive multi-omics profiling analysis. *Sci Total Environ*. 2024;919:170869. doi:10.1016/j.scitotenv.2024.170869
24. Bouchama A, Rashid M, Malik SS, et al. Whole genome transcriptomic reveals heat stroke molecular signatures in humans. *J Physiol*. 2023;601 (12):2407–2423. doi:10.1113/JP284031
25. Mughal W, Martens M, Field J, et al. Myocardin regulates mitochondrial calcium homeostasis and prevents permeability transition. *Cell Death Differ*. 2018;25(10):1732–1748. doi:10.1038/s41418-018-0073-z
26. Zhang XH, Wu JX, Sha JZ, Yang B, Sun JR, Bao ED. Heat shock protein 90 relieves heat stress damage of myocardial cells by regulating Akt and PKM2 signaling in vivo. *Int J Mol Med*. 2020;45(6):1888–1908. doi:10.3892/ijmm.2020.4560
27. Li Y, Liu X. The inhibitory role of Chinese materia medica in cardiomyocyte apoptosis and underlying molecular mechanism. *Biomed Pharmacother*. 2019;118:109372. doi:10.1016/j.biopha.2019.109372
28. Crow MT, Mani K, Nam YJ, Kitsis RN. The mitochondrial death pathway and cardiac myocyte apoptosis. *Circ Res*. 2004;95(10):957–970. doi:10.1161/01.RES.0000148632.35500.d9
29. Yang Y, Li C, Xiang X, et al. Ursolic acid prevents endoplasmic reticulum stress-mediated apoptosis induced by heat stress in mouse cardiac myocytes. *J Mol Cell Cardiol*. 2014;67:103–111. doi:10.1016/j.yjmcc.2013.12.018
30. Chen Y, Jiang W, Liu X, et al. Curcumin supplementation improves heat-stress-induced cardiac injury of mice: physiological and molecular mechanisms. *J Nutr Biochem*. 2020;78:108331. doi:10.1016/j.jnutbio.2019.108331
31. Wu F, Gao F, He S, Jiang Y, Luo G, Xiao Y. c-Jun promotes the survival of H9c2 cells under hypoxia via PTEN/Akt signaling pathway. *J Physiol Biochem*. 2019;75(4):433–441. doi:10.1007/s13105-019-00695-3
32. Wisdom R, Johnson RS, Moore C. c-Jun regulates cell cycle progression and apoptosis by distinct mechanisms. *EMBO J*. 1999;18(1):188–197. doi:10.1093/emboj/18.1.188
33. Meng Q, Xia Y. c-Jun, at the crossroad of the signaling network. *Protein Cell*. 2011;2(11):889–898. doi:10.1007/s13238-011-1113-3
34. Liu J, Lin A. Role of JNK activation in apoptosis: a double-edged sword. *Cell Res*. 2005;15(1):36–42. doi:10.1038/sj.cr.7290262
35. Chen F. JNK-induced apoptosis, compensatory growth, and cancer stem cells. *Cancer Res*. 2012;72(2):379–386. doi:10.1158/0008-5472.CAN-11-1982
36. Ryan TA, Roper KM, Bond J, Bell SM, Sweeney ST, Morrison EE. A MAPK/c-Jun-mediated switch regulates the initial adaptive and cell death responses to mitochondrial damage in a neuronal cell model. *Int J Biochem Cell Biol*. 2018;104:73–86. doi:10.1016/j.biocel.2018.09.008
37. Mhone TG, Chen MC, Kuo CH, et al. Daidzein synergizes with gefitinib to induce ROS/JNK/c-Jun activation and inhibit EGFR-STAT/AKT/ERK pathways to enhance lung adenocarcinoma cells chemosensitivity. *Int J Biol Sci*. 2022;18(9):3636–3652. doi:10.7150/ijbs.71870
38. Wei H, Wang H, Wang G, et al. Structures of p53/BCL-2 complex suggest a mechanism for p53 to antagonize BCL-2 activity. *Nat Commun*. 2023;14(1):4300. doi:10.1038/s41467-023-40087-2
39. Zhang Y, Wu Q, Bai F, et al. Granulosa cell-specific FOXJ2 overexpression induces premature ovarian insufficiency by triggering apoptosis via mitochondrial calcium overload. *J Ovarian Res*. 2025;18(1):75. doi:10.1186/s13048-025-01651-0
40. Kitamura C, Ogawa Y, Nishihara T, Morotomi T, Terashita M. Transient co-localization of c-Jun N-terminal kinase and c-Jun with heat shock protein 70 in pulp cells during apoptosis. *J Dent Res*. 2003;82(2):91–95. doi:10.1177/154405910308200203
41. Sawai M, Ishikawa Y, Ota A, Sakurai H. The proto-oncogene JUN is a target of the heat shock transcription factor HSF1. *FEBS J*. 2013;280 (24):6672–6680. doi:10.1111/febs.12570